Korean J. Chem. Eng., **28**(3), 778-787 (2011)
DOI: 10.1007/s11814-010-0421-2

Combustion gas and NO emission characteristics of hazardous waste mixture particles in a fixed bed

Ling Tao*,,†, Guangbo Zhao*, and Rui Sun***

*School of Energy Science and Engineering, Harbin Institute of Technology,
92, West Dazhi Street, Harbin 150001, P. R. China
**Qingdao Huashijie Environ. Prot. Technol. Co., Ltd., NO 16, Liupanshan Rd., Qingdao, Shandong, P. R. China
(*Received 11 January 2010 • accepted 4 September 2010*)

Abstract−Experiments with fixed-bed incinerators were carried out to model the combustion characteristics and gas emission characteristics of hazardous waste mixture particles in a grate furnace. The results indicate that combustion can be divided into three stages: ignition, main combustion and combustion completion stage. According to the various concentrations of O_2, CO_2 and CO, the main combustion stage can be subdivided into pyrolysis gas combustion and char combustion. Primary air rate, moisture and particle size have significant effects on concentrations of combustion gases and NO. Bed height has no effect on CO_2 concentrations but does have an effect on other combustion gases and NO emissions.

Key words: Fixed Bed, Hazardous Waste, Combustion Characteristics, Combustion Gas Concentration, NO Emission

INTRODUCTION

Hazardous waste from industrial production is becoming an increasing issue. Incineration is widely used for its ability to minimize and disinfect waste and low production levels of secondary pollution [1-4]. Hong Chen studied detailed polychlorinated biphenyls (PCBs) congener patterns in the flue gas from a medical waste incinerator (MWI) using high-resolution gas chromatograph coupled to high-resolution mass spectrometer (HRGC/HRMS). The total PCBs concentration in the flue gas ranged from 138.01 to 855.35 ng/Nm^3 under different operating conditions. Three inhibitors, sulfur, urea, and ammonium sulfate, were tested to investigate the capacity for preventing PCBs formation. Urea mixed with ammonium sulfate and more activated carbon was the most effective inhibitor for PCBs formation [5]. Liu took the sulfur solidification technology into the incineration of industrial hazardous wastes, in order to decrease the SO_2 concentration in the flue gas [6]. Guan thought controlling the pollutants generated by hazardous waste incineration during they are forming was as important as dealing with them after they had formed [7]. She presented an idea of controlling the amount of pollutants generated by during the incineration of hazardous waste through adjusting the combustion conditions [7].

To optimize combustion and produce less pollution, combustion characteristics and gas release of grate furnace need to be studied. A fixed bed is widely used in investigating the combustion in a grate furnace and stationary grate boilers by transforming the combustion on the grate to a one-dimensional reactor. The fuel of the reactor could be coals, municipal solid wastes, medical wastes and biomass materials [8]. Waste properties and incineration conditions, such as fuel type, particle size, moisture and primary air rate, impact the combustion characteristics by changing the heat generation, heat transfer and reaction rates in a very complicated way. Combustion characteristics of municipal solid wastes, biomass and medical wastes have already been studied [9-13]. Nevertheless, gas releases and NO emissions of industrial hazardous wastes are seldom studied. To study the gas release and pollution in a grate furnace, a one-dimensional test assembly is used to model the combustion in the grate furnace. Gas releases and NO emissions of industrial hazardous wastes are also investigated. Gas releases and NO emissions of different primary air rate, moisture, bed height and particle size are discussed.

†To whom correspondence should be addressed.
E-mail: taolingsd@yahoo.com.cn

EXPERIMENTAL

1. Combustion in a Grate Furnace and the Description of Fixed Bed

Fig. 1 presents a schematic diagram of the combustion phases in a grate furnace. The waste pushed into the furnace by a feeder forms a uniform bed on the grate. It is then transported horizontally by an endless chain grate. As the waste burns in the furnace, the waste bed is divided into four zones by temperature: 1) preheating and drying zone, 2) volatile devolatilization and combustion zone, 3)

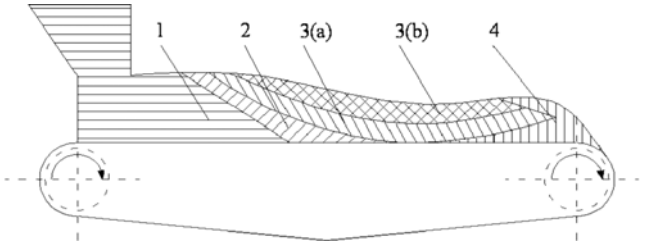

Fig. 1. The combustion zones on a grate furnace.
1. Preheating and drying zone
2. Volatile devolatilisation and combustion zone
3(a). Char reduction zone
3(b). Char oxidation zone
4. Ash residue burning-out zone

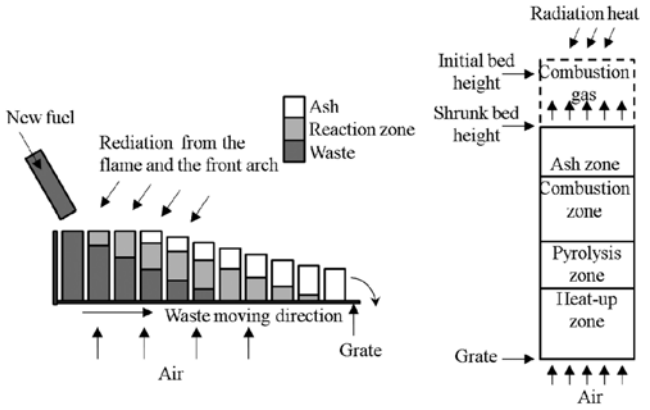

Fig. 2. The model process of the waste combustion in a grate furnace.

char combustion zone, and 4) ash residue burning-out zone. Radiation from the flame above the bed and the hot front arch immediately heats the waste bed, thereby forming the preheating and drying zone. The dried waste then releases volatile, which consists of CH_4, CO, CO_2, NH_3, H_2O, some other light alkanes and tar. The volatile starts burning above the bed surface and the flame irradiates the waste bed, creating the volatile devolatilization and combustion zone. Subsequently, char in the waste bed starts to burn, which causes the highest temperatures in the bed. This establishes the char combustion zone that can be further divided into two subzones. With a supply of air from the bottom, the char at the bottom burns in an oxygen-rich atmosphere, forming a waste layer of char oxidation. Char at the top of the bed resides in an oxygen-poor atmosphere. Meanwhile, flue gas from char oxidation rises through the bed to the top, chemically reducing and depositing a layer of char reduction. Finally, a little char remains burning within an ash deposit that constitutes the ash residue burning-out zone.

One way to visualize the whole process is taking a fixed columnar cross-section in the waste bed and following its constitutive profile as it is transported on the chain grate. The time development of this profile within the column corresponds to the horizontal motion of the chain grate in the continuous process. In essence, primary air and combustion gases move upwards, while waste moves horizontally. As the reaction progresses, evaporation, pyrolysis and combustion are initiated at the top surface of the bed and then proceed downward. The waste in the column experiences a sequential process of heating, water evaporation, pyrolysis, gas combustion, and char combustion. While the waste bed moves very slowly, spending one hour or even longer on the grate, primary air and combustion gases pass through the waste bed in several seconds. Hence, the temperature and concentration gradients of chemical species in the direction of the waste bed motion are negligible compared with those in the direction of gas flow, indicating that horizontal heat and mass transfers can be ignored. Based on the above description, continuous and steady combustion of the waste on the grate can be simulated by a one-dimensional model, as depicted in Fig. 2 [14]. The waste bed in a grate furnace is modeled as a layer of waste particles with similar physical and chemical characteristics. Primary air flows upwards from the bottom. Volatiles, combustion gases and flue gas move upward in the same direction by primary air.

Table 2. Experimental conditions

No.	Primary air rate	Moisture	Ash	Height	Particle size
	Nm^3/h	%	%	mm	mm
1	4	19.98	28.60	500	50
2	6	19.34	28.83	500	50
3	10	20.15	28.54	500	50
4	14	20.80	28.31	500	50
5	18	20.70	27.63	500	50
6	14	25.93	26.48	500	50
7	14	15.93	30.05	500	50
8	14	12.57	31.25	500	50
9	14	20.87	28.28	300	50
10	14	20.87	28.28	400	50
11	14	21.63	28.01	600	50
12	14	21.73	27.26	500	20
13	14	21.47	27.35	500	30
14	14	20.22	28.51	500	40

2. Specimen and Experimental Conditions

The Shanghai LüZou Environmental Protection Engineering Company provided specimens of hazardous wastes. The composition of these specimens included paint slag (24%), tar slag (27%), emulsion slag (29%), Ca $(OH)_2$ (13%) and paper (7%). Paint slag, tar slag and emulsion slag are high heating value hazardous wastes, whose numbers in the State Hazardous Waste List are HW12, HW09 and HW11, respectively. Paper simulates low heating value waste. Ca $(OH)_2$ simulates inorganic matters.

Mixtures of these wastes were ground into small pieces and extruded into particles with a roller-forming machine. The properties of waste mixtures and experimental conditions are listed in Tables 1 and 2, respectively. The primary air rate, the bed height and particle size varied from 4 to 18 Nm^3/h, from 300 to 600 mm and from 20 to 50 mm, respectively. The moisture of the waste was changed by evaporating part of the moisture in a drying machine at 60, 70, 80 and 90 °C for 8 hours.

3. Experimental System and Measuring Instrument

Fig. 3 shows a schematic diagram of the experimental facility. The facility consists of a cylindrical combustion chamber, gas burner and gas supply system, grate, air supply system, temperature measuring system, combustion gas sampling and measuring system, and weight measuring system. The height of the cylindrical chamber is 1,500 mm and the inner diameter is 180 mm. The chamber is made of 50 mm thick high-alumina refractory material that can withstand temperatures up to 1,300 °C, 5 mm thick protective casing of 1Cr18Ni9Ti steel and 150 mm thick insulation made of alumi-

Table 1. Composition and thermal characteristics of waste

M_{ar} (%)	A_{ar} (%)	V_{daf} (%)	C_{ar} (%)	H_{ar} (%)	O_{ar} (%)	N_{ar} (%)	S_{ar} (%)	$Q_{net,\,ar}$ (kJ/kg)
33.49	23.77	81.14	28.83	3.17	10.63	0.07	0.04	10145

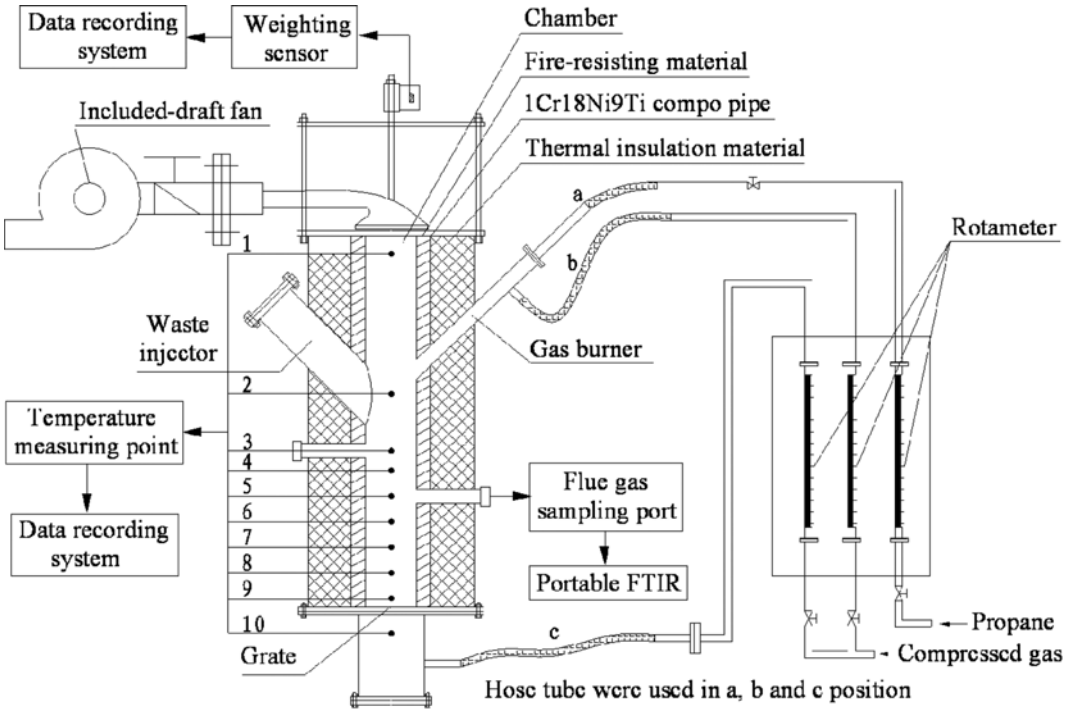

Fig. 3. Schematic diagram of the one-dimensional experimental facility.

num silicate refractory fiber from the inner to the outer layer. The grate, located at the bottom of the chamber, is a circular disc made from stainless steel with a diameter of 178 mm, and has 96 concentrically-arranged holes each of 7 mm diameter, making an open area of 14.8%. A gas burner is installed at 45° to the sidewall at 750 mm above the grate to ignite the waste. It models the radiation from front arch and gas combustion. A tank of compressed air supplies primary air and air needed to mix with propane. The flow rates of air and propane are monitored by rotameters. The primary air is fed into the chamber without preheating from the bottom through the grate. Ten thermocouples, labeled tc1 to tc9, are arranged along the chamber's longitudinal axis; positions are presented in Table 3. The thermocouples measure temperatures of the flue gas (tc1), the propane flame (tc2), combustion gas above the bed (tc3) and waste bed (tc4-tc9), while thermocouple tc10 is placed under the grate to measure primary air temperatures. An included-draft fan is used to drive out flue gas in the chamber. The whole chamber is suspended with a weighing scale monitoring the weight loss during each experimental run. To avoid weight measuring errors, flexible gas tube junctions are used. A combustion gas sampling port mounted on the side wall at 388 mm above the grate is connected with a portable FTIR.

In the course of each experimental run, various measuring systems have been used to record temperature, weight and gas composition. The temperature-measuring equipment includes ten thermocouples connected to a temperature monitoring system. The weight measuring equipment includes a weighing sensor and a weighing scale. The gas composition equipment includes a sampling probe, a set of gas cleaning devices and a portable FTIR. The portable FTIR has a wavelength range of 900-4,200 cm^{-1}, resolution 8 cm^{-1}, gas cell volume of 1.07 L, gas cell and pipe temperature of 180 °C, and a scanning speed of 10 Hz. Combustion gas spectra are obtained while gas is pumped into the gas cell. Spectra are then analyzed by software provided with the portable FITR. Gas concentrations and spectra can be digitally stored for post analysis. In this work, the evolution of CO, CO_2, CH_4, NO and O_2 concentrations with different primary air rate, moisture, bed height and particle size is our primary focus.

Before commencing experimental runs, preparations included calibrating the weighing scale and inserting specimens into the chamber through the waste injector, which is then locked to separate air and heat. With the preparations completed, propane is ignited and the chamber temperature rises rapidly to 900 °C. The propane flow is then adjusted to maintain a steady temperature. The high temperature flame immediately irradiates the waste bed, from which point data starts to be measured and recorded. At the moment that the gas-phase fire can be observed visibly, primary air is set flowing into the chamber, slowly at first, but subsequently increased until the desired rate is reached.

Table 3. The positions of ten thermocouples

No.	1	2	3	4	5	6	7	8	9	10
Height* (mm)	1238	748	548	478	388	298	208	118	28	−90

*Height means the distance from the corresponding thermocouple to the grate

RESULTS AND DISCUSSION

1. NO Concentration Calculation Method

As mentioned above, NO concentrations in the combustion gas are measured by the portable FTIR. However, different flue gas volumes and the same NO concentration leads to different levels of

NO emission. For this reason, the method to calculate NO concentrations for pulverized coal boilers is not suitable for grate furnaces or fixed beds. A new method has to be proposed to evaluate NO emission level in such cases. By introducing a flue gas volume, we can reanalyze the method by which NO evaluation is performed. This is done below.

Mass balance is maintained during the entire combustion process; that is, the mass of primary air and fuel before combustion equals the mass of flue gas and ash residue. This can be expressed by the following equation.

$$dM_{air}+dM_{fuel}=dM_{flue\ gas}+dM_{ash\ residue} \quad (1)$$

Subtracting $dM_{ash\ residue}$ from both side of above equation, the following equation can be obtained:

$$dM_{air}+(dM_{fuel}-dM_{ash\ residue})=dM_{flue\ gas} \quad (2)$$

where the difference $(dM_{fuel}-dM_{ash\ residue})$, which can be denoted by ΔM, represents the weight loss during the combustion process. The value of ΔM can be calculated by the following equation:

$$\Delta M=(dM_{fuel}-dM_{ash\ residue})=S\cdot v \quad (3)$$

S is the area of the grate (m^2) and v is the burning rate of the combustion ($kg/(m^2\cdot min)$).

The quantity dM_{air} is the mass flow of primary air supplied from the bottom of the furnace. The relationship between the mass flow and the volume flow of primary air is given in the following.

$$dM_{air}=\frac{G}{60}\cdot\rho \quad (4)$$

G is the volume flow of the primary air (Nm^3/h) and ρ is the density of the air at room temperature (kg/Nm^3). Thus, the mass of the flue gas can be obtained.

$$dM_{flue\ gas}=S\cdot v+\frac{G}{60}\cdot\rho \quad (5)$$

We can now define the NO concentration in either grate furnaces or fixed beds as follows:

$$[NO]_{t_1-t_2}=\frac{\int_{t_1}^{t_2}\left(S\cdot v+\frac{G}{60}\cdot\rho\right)[NO]_{meas}dt}{\int_{t_1}^{t_2}\left(S\cdot v+\frac{G}{60}\cdot\rho\right)dt} \quad (6)$$

$[NO]_{meas}$ is the measured concentration of NO (mg/m^3) and $[NO]_{t1-t2}$ is the average NO concentration between t_1 and t_2 (mg/m^3), while t_1 and t_2 are, respectively, the initial and final recording times over which the NO average concentrations are measured.

2. The Combustion Characteristics of the Fixed Bed

Temperatures above and within the bed are shown in Fig. 4. Temperature at tc2 rises quickly to 900 °C and remains there during the whole experiment. Due to radiation from the propane flame, temperatures over the bed (tc3) and on the bed surface (tc4) start to rise immediately. From this moment, waste at the surface starts to dry out and pyrolyze. Pyrolysis gas is released from the bed and burns directly above the bed. Meanwhile, evaporation and pyrolysis start in the lower layer. After ignition, these reactions descend through the bed at a fixed speed. After a while, temperatures at tc5 start to rise, measured by the highest thermocouple within the bed layer,

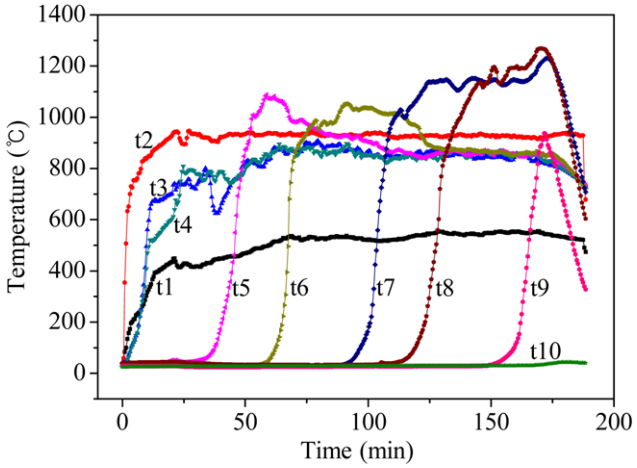

Fig. 4. The temperature distribution upon and in the waste bed for case 4.

indicating steady combustion in the bed.

Two further observations should be noticed. First, the highest temperatures of tc7 and tc8 are much higher than those of tc5 and tc6. This can be explained in the following manner. In the steady-combustion period, char produced before this moment and gas produced at this moment combust at the same time. However, there is not enough oxygen to fuel complete combustion of both. Pyrolysis gases released in a layer lower than char, signifying that pyrolysis gases burn first. Hence, these gases burn until depleted, while char burns slowly at a lower temperature because of the lack of oxygen. After a while, most of pyrolysis gases release and then burn out and a large quantity of char accumulates in the bottom of the chamber. Without the presence of pyrolysis gases, all oxygen is now consumed in char combustion, greatly increasing the burning rate of the char. The result is an increase in temperatures of tc7 and tc8.

The second observation is that the highest temperature of tc9 is lower than the highest temperatures measured by other thermocouples in the bed. This is caused by the cooling effect of primary air. The temperature of flue gas is also presented in Fig. 4. The temperature of tc1 rises immediately to more than 400 °C after propane ignition, and increases a little further to 500 °C after the waste

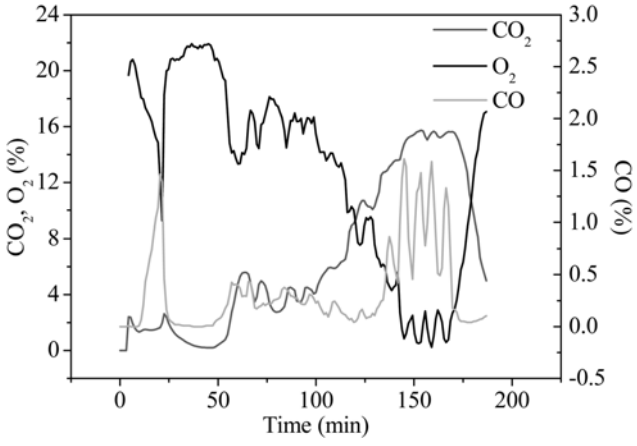

Fig. 5. The concentration of CO_2, CO and O_2 during the experiment.

starts burning. The weight loss of the bed during this period is shown in Fig. 4. The combustion process is divided into three stages: first, an ignition stage with a different slope to the steady weight loss rate; second, a period with steady weight loss rate; and third, a period when reactants are spent, characterized by diminishing weight loss rates.

Concentrations of CO_2, CO and O_2 are presented in Fig. 5. The gas distributions can also be divided into three stages. The first stage corresponds to the ignition of the waste bed. In this stage, CO levels increases and then decreases rapidly. At the same time, O_2 levels take a very sharp decline and subsequent upsurge, while CO_2 attains a small peak. In explanation, before the gas-phase combustion, pyrolysis gases release and gather above the bed, at which point, primary air has not yet been supplied. The propane flame and its accompanying downward flowing air causes pyrolysis gases to flow down into the bed. The gas sampling system pumps out only pyrolysis gases as there are no other gases in the bed at this stage. However, a short time later, pyrolysis gases start to burn and a supply of primary air begins. Air from the bottom is pumped into the gas sampling system. Hence, a short time period of little CO and CO_2 and more than 20% O_2 is observed in concentrations displayed in Fig. 5.

The second stage is the main time period characterized by pyrolysis gas combustion when O_2 decreases and CO_2 increases. In this stage, most of O_2 is consumed in pyrolysis gas combustion producing large quantities of CO_2. CO remains at low levels, because little of the available O_2 is retained for char combustion in this period. The third stage is dominated by char combustion where the O_2 is almost depleted and CO levels suddenly rise. In this stage, most of pyrolysis gases have burnt out. Large amounts of char left in the second stage start to burn at a fast rate requiring much more O_2. Primary air is in short supply in this combustion stage, and consequently, a large quantity of CO forms in the process. Finally, all combustible material burns out. CO_2 and CO are found to decrease rapidly, while O_2 increases rapidly.

Wave fronts are observed in measurements of gas levels. This can be explained by the fact that waste particle sizes are approximately 50 mm, and there are a finite number of particles in the bed. Each particle undergoes combustion independent of others and moreover at different stages. Thus, gas release in the whole bed is not steady.

Mass balances are made over the collected gases and the ash residue in the dust bunker. The composition of the ash residue is presented in Table 4. As far as C, O and N are concerned, about additional 2.21% of the initial carbon is found, whereas 13% of the initial N and 11% of the initial oxygen are missing. However, the mass balance of hydrogen cannot be obtained, because water vapor which is formed by hydrogen is absorbed by the gas cleansing system and cannot be measured in the gas. From the viewpoint of carbon conversion, the mass balance of the experiments closes satisfactorily.

4. Effect of Primary Air Rate on Combustion Gases and NO Emissions within the Bed

Combustion gases we focus on are CO, CO_2, CH_4 and O_2, concentrations of which are given as averages of the whole combustion process. The variation of CO_2 and CO concentrations with respect to primary air rate is presented in Fig. 6(a) and Fig. 6(b), respectively. Black squares represent experimental results and red lines are fitting curves of these results. Clearly, the average CO_2 concentration increases at first, reaches a peak value at 14 Nm^3/h and subsequently decreases. The average CO concentration decreases with increasing primary air rate and is roughly equal at 14 Nm^3/h and 18 Nm^3/h. Increases in CO_2 and decreases in CO mainly occur in char combustion stage. In pyrolysis combustion stage, O_2 for combustion is plentiful and most of carbon in the pyrolysis gas forms CO_2, producing a little CO. Levels of CO_2 and CO are roughly the same in this stage. In the char combustion stage, depleted O_2 levels result in incomplete combustion of char and thus promote CO formation. An increase in primary air rate encourages formation of more CO_2 and less CO. At primary air rate of 14 Nm^3/h, wastes in the bed are completely burned, thereby attaining the highest CO_2 concentration and lowest CO concentration. Further increases in primary air rate supplies too much air into the furnace and dilutes combustion gases. Another contributing aspect is that too high primary air rate cools the furnace and decreases the burning rate, thereby increasing CO formation and decreasing CO_2 formation.

The effect of primary air rate variation on average O_2 concentration is shown in Fig. 6(c). Clearly, average O_2 concentration increases with increasing primary air rate. In pyrolysis gas combustion stage, O_2 consumption remains constant and with higher primary air rates; a surplus of O_2 appears in this stage. In char combustion stage, all O_2 is consumed. The increase in O_2 with increasing primary air rate is mainly due to the higher concentration of O_2 in the pyrolysis gas combustion stage.

The dependence of CH_4 average concentrations on primary air rates is shown in Fig. 6(d). After initially decreasing, CH_4 concentration reaches a minimum value and subsequently rises. The burning rate of combustion greatly affects CH_4 concentration. At low primary air rates, the burning rate is low as pyrolysis gases cannot completely burn due to O_2 lack. Thus, CH_4 concentration is high. With an increase in the primary air rate, burning rate rises. An adequate supply of O_2 promotes an earlier and faster burn of CH_4; hence, CH_4 concentration is low. At a primary air rate of 18 Nm^3/h, the burning rate decreases because of primary air cooling. Released CH_4 cannot burn sufficiently well; thus concentrations of the gas rise again.

The average NO concentrations of the whole combustion process for different primary air rates are presented in Fig. 6(e). From the figure, a minimum in the NO concentration occurs at 10 Nm^3/h. Higher or lower primary air rates cause high NO concentrations. Temperatures within the furnace are higher than 800 °C but lower than 1,200 °C associated with the NO formation regime. Hence, NO concentrations depend on reduction of NO and combustion gas, indicating that more reduction equates with less NO emissions. CO and CH_4 are main reducers in these reduction reactions. At low primary air rates, CO and CH_4 concentrations are high but reduction rates are very low because of low furnace temperatures. With increasing primary air rate, furnace temperatures rise in parallel with reduction rates. However, at primary air rates of 14 and 18 Nm^3/h, low CO and CH_4 levels subsist to advance any reduction. NO concentrations at these rates return to higher values.

Table 4. Composition of the ash residue

M_{ar} (%)	A_{ar} (%)	V_{ar} (%)	FC_{ar} (%)	C_{ar} (%)	H_{ar} (%)	O_{ar} (%)	N_{ar} (%)	S_{ar} (%)
0.26	96.09	3.23	0.42	3.10	0.54	0.00	0.00	0.01

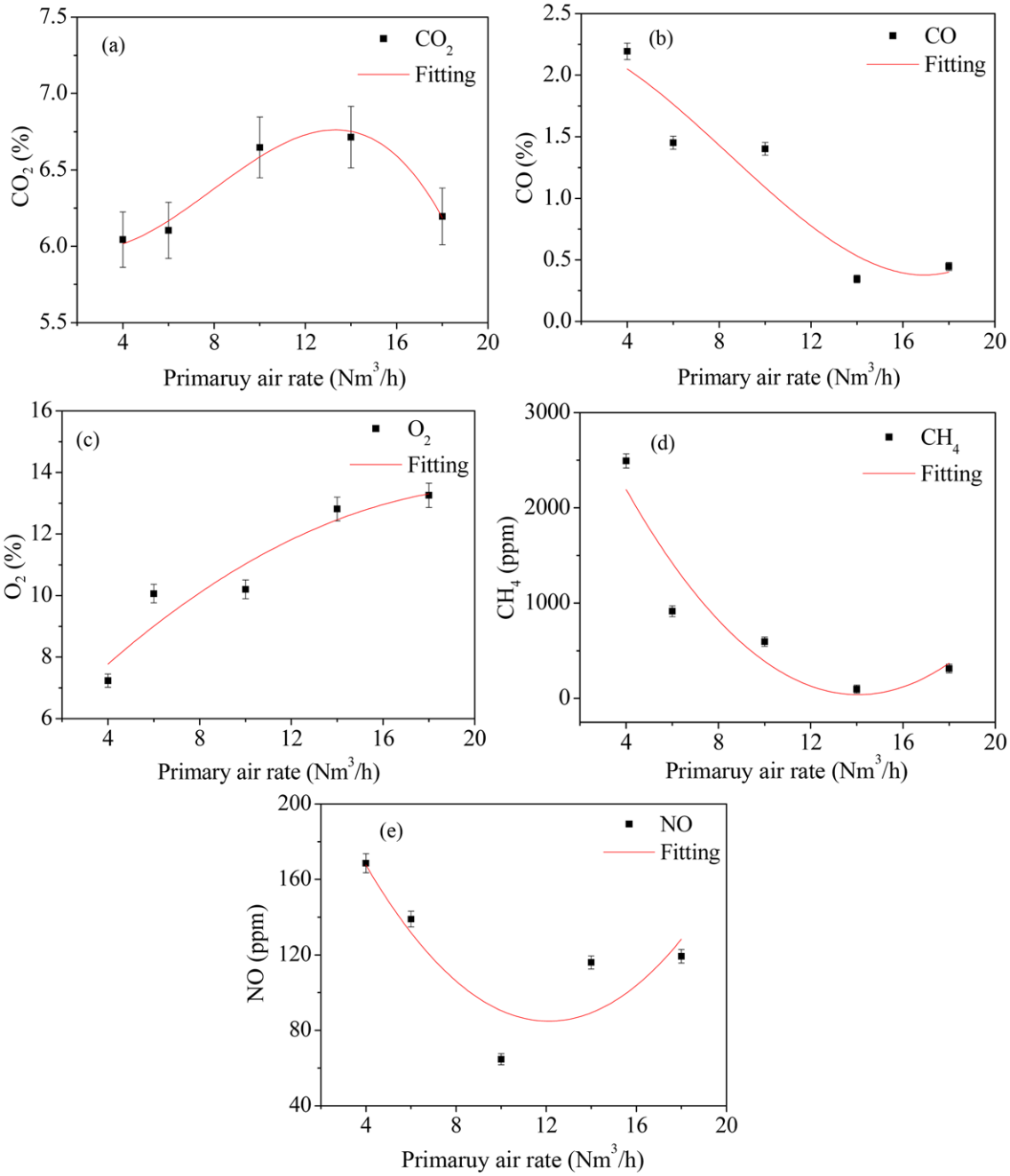

Fig. 6. The effect of primary air rate on combustion gases and NO.

5. Effect of Moisture on Combustion Gases and NO Emissions in the Bed

Dependence of CO_2, CO and O_2 concentrations on moisture content is relatively simple, as seen in Figs. 7(a), 7(b) and 7(c), respectively. From the figures, we can see that CO and CO_2 concentrations decrease, while O_2 concentrations increase with increasing moisture. Wastes with different moisture content and same quality have different carbon content. Waste of higher moisture has lower carbon content, which in the combustion process leads to less CO and CO_2 being produced. This also leads to more O_2 present in the combustion gas. Fig. 7(d) shows the variation of CH_4 concentration with moisture content. Concentrations decrease with increasing moisture content as combustible materials in the waste increase.

NO concentration trend with respect to moisture content is shown in Fig. 7(e). These also decrease with increasing moisture content. As amounts of combustible material in the waste decrease with increasing moisture content, NO production also decreases.

6. Effect of Bed Height on Combustion Gases and NO Emission within the Bed

The effect of bed height on CO_2 average concentration is shown in Fig. 8(a). Here, CO_2 concentration exhibits little variation because in the main combustion stage of these four test settings, fuel properties and combustion conditions are similar. Waste then burns under like situations, and hence CO_2 formations are at the same level. Aver-

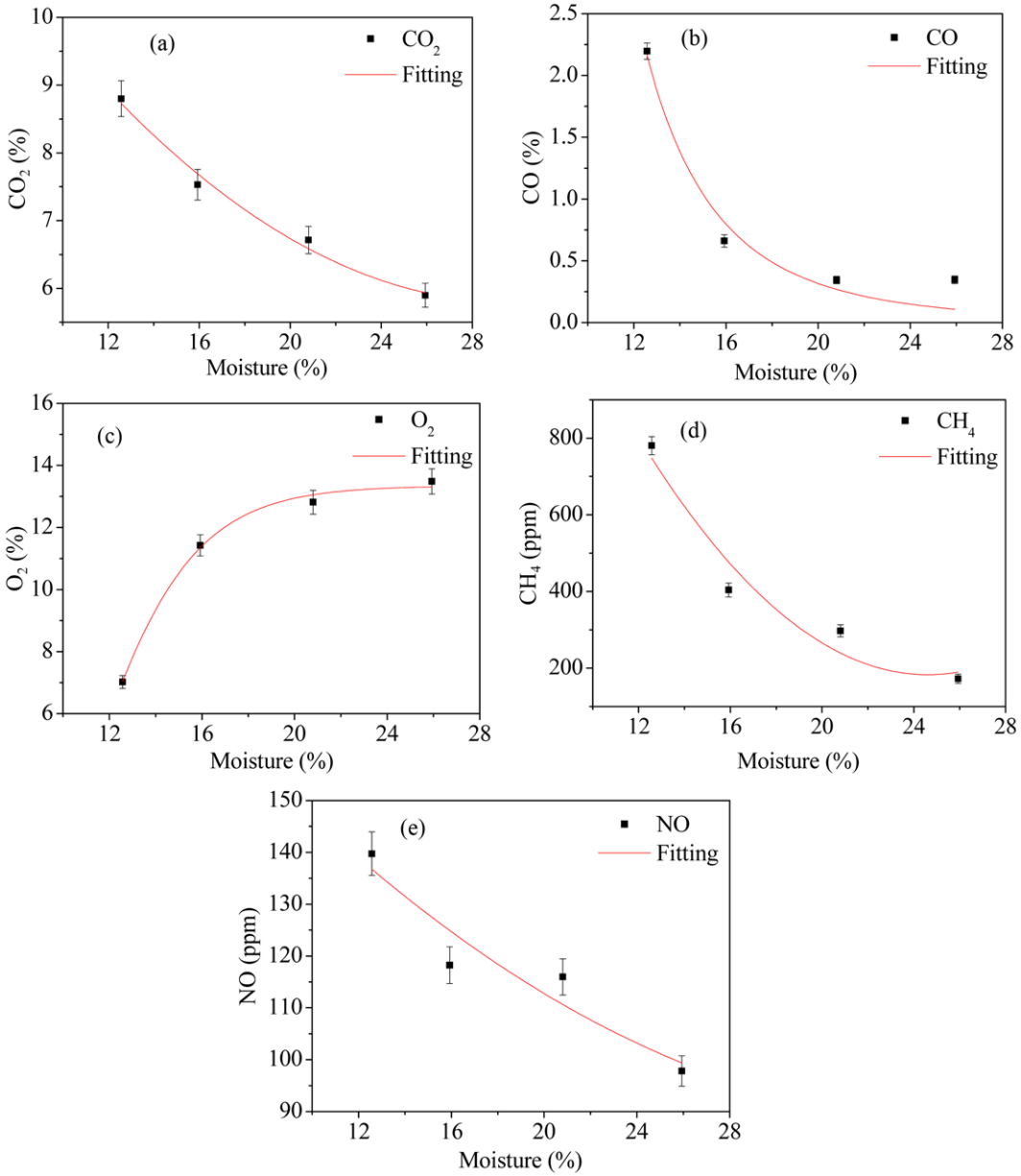

Fig. 7. The effect of moisture on combustion gases and NO.

age concentrations of CO for different bed heights are presented in Fig. 8(b). All CO concentrations are observed to be at a lower level compared with those conditions with different primary air rates. The explanation is that wastes for these four different bed heights burn in an oxygen-rich atmosphere. Most of the carbon in the waste reverts to CO_2, except in the ignition stage and in the char combustion stage when a large amount of CO is released. CO concentration decreases with the increase of bed height. In pyrolysis gas combustion stage, little CO is produced. CO mostly forms in the ignition stage and char combustion stage. In the later stage, CO is produced at the same level for different bed heights because combustion conditions remain the same. However, CO levels formed in the ignition stage are not at the same levels. In the ignition stage, lower bed height results in less irradiation on the surface of the bed, slowing heating. Sufficient quantities of CO are released. In addition, there is no O_2 to fuel the conversion of CO to CO_2. Thus, for low bed heights, CO concentration is high.

O_2 concentration, as displayed in Fig. 8(c), increases with increasing bed height. In pyrolysis gas combustion stage, adequate O_2 supply does exist for combustion, indicating a surplus in O_2 after combustion. However, in char combustion stage, no O_2 remains. The average concentration of O_2 is the average O_2 concentrations of these stages. Conditions with high bed heights give rise to a long pyrolysis-gas combustion stage, which means higher average O_2 concentrations.

The trend in average CH_4 concentration for different bed heights is shown in Fig. 8(d). CH_4 concentration is observed to decrease with bed height. Most of the CH_4 is released before the ignition of the bed. Conditions with low bed height require more time to attain ignition, thereby extending the time for CH_4 release. Hence, lower

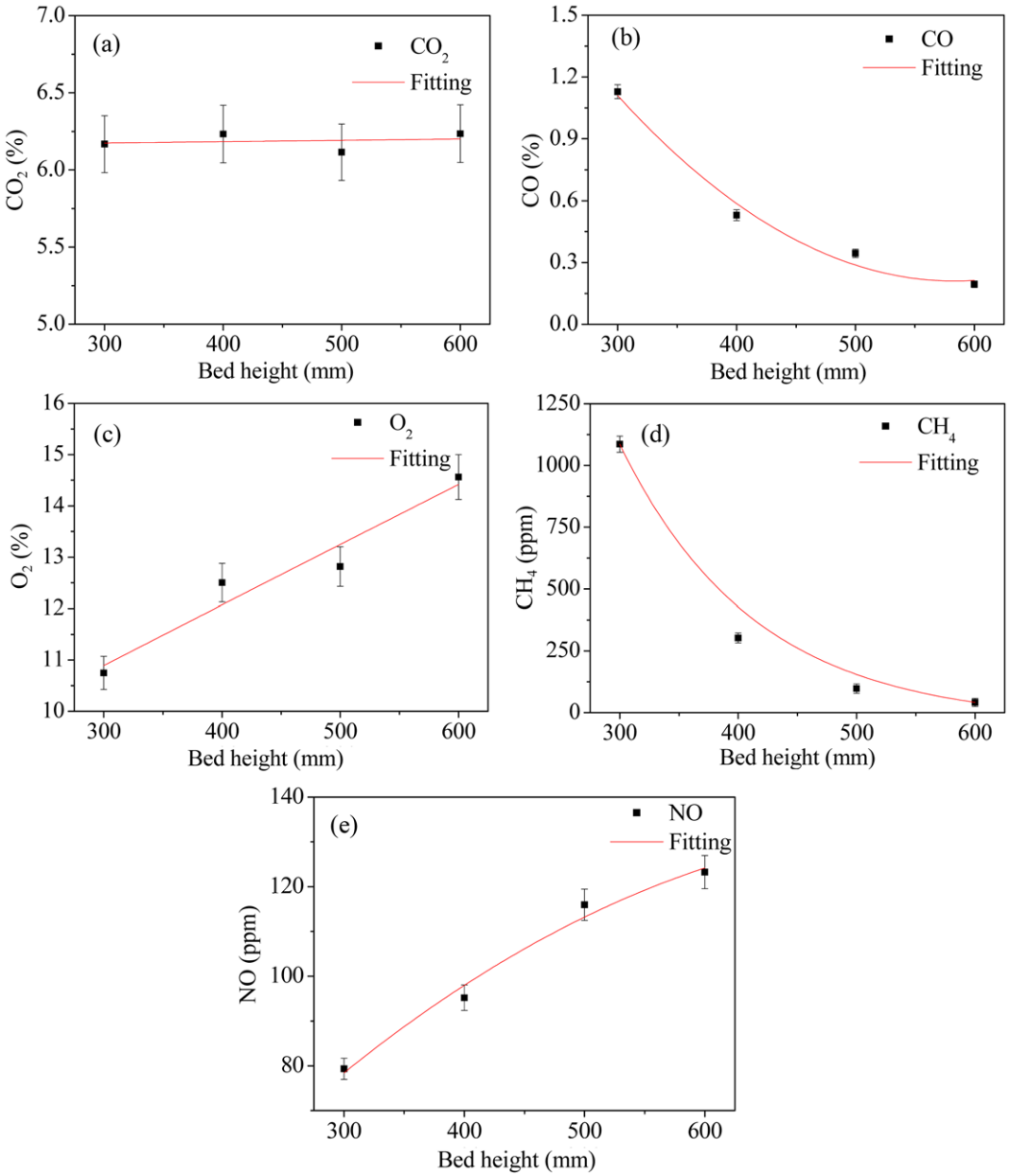

Fig. 8. The effect of bed height on combustion gases and NO.

bed heights imply higher CH_4 concentrations.

Average NO concentrations for different bed height are shown in Fig. 8(e). From the figure, NO concentration increases with increasing bed height. This is in contrast to the behavior seen in Figs. 8(b) and 8(d), where CH_4 and CO decrease. Lower levels in CO and CH_4 imply corresponding declines in NO reduction, i.e., more NO remains in the flue gas.

7. Effect of Particle Size on Combustion Gases and NO Emission within the Bed

Average concentrations of CO_2, CO, O_2 and CH_4 for different particle sizes are shown in Figs. 9(a), 9(b), 9(c) and 9(d), respectively. Average concentrations of CO_2 increase nearly linearly and those of CO and CH_4 decrease with increasing particle size. Larger particles have enormous temperature gradients between surface and core. Waste in the core of these particles is at a much lower temperature, which slows the release of CO and CH_4. This explains why levels of these molecules decrease with increasing particle size. However, more carbon is converted to CO_2 in the pyrolysis gas combustion stage. Hence, conditions with larger particles have high CO_2 concentrations but low O_2 concentrations.

Variation of the average NO concentration with particle size is shown in Fig. 9(e). NO concentrations increase with increasing particle size. This can be easily explained in light of decreases in CH_4 and CO discussed above, where reductions weaken and more NO remains in the flue gas.

CONCLUSIONS

A new method of calculation is proposed to evaluate NO emission levels in grate furnaces and fixed beds. A flue gas volume was

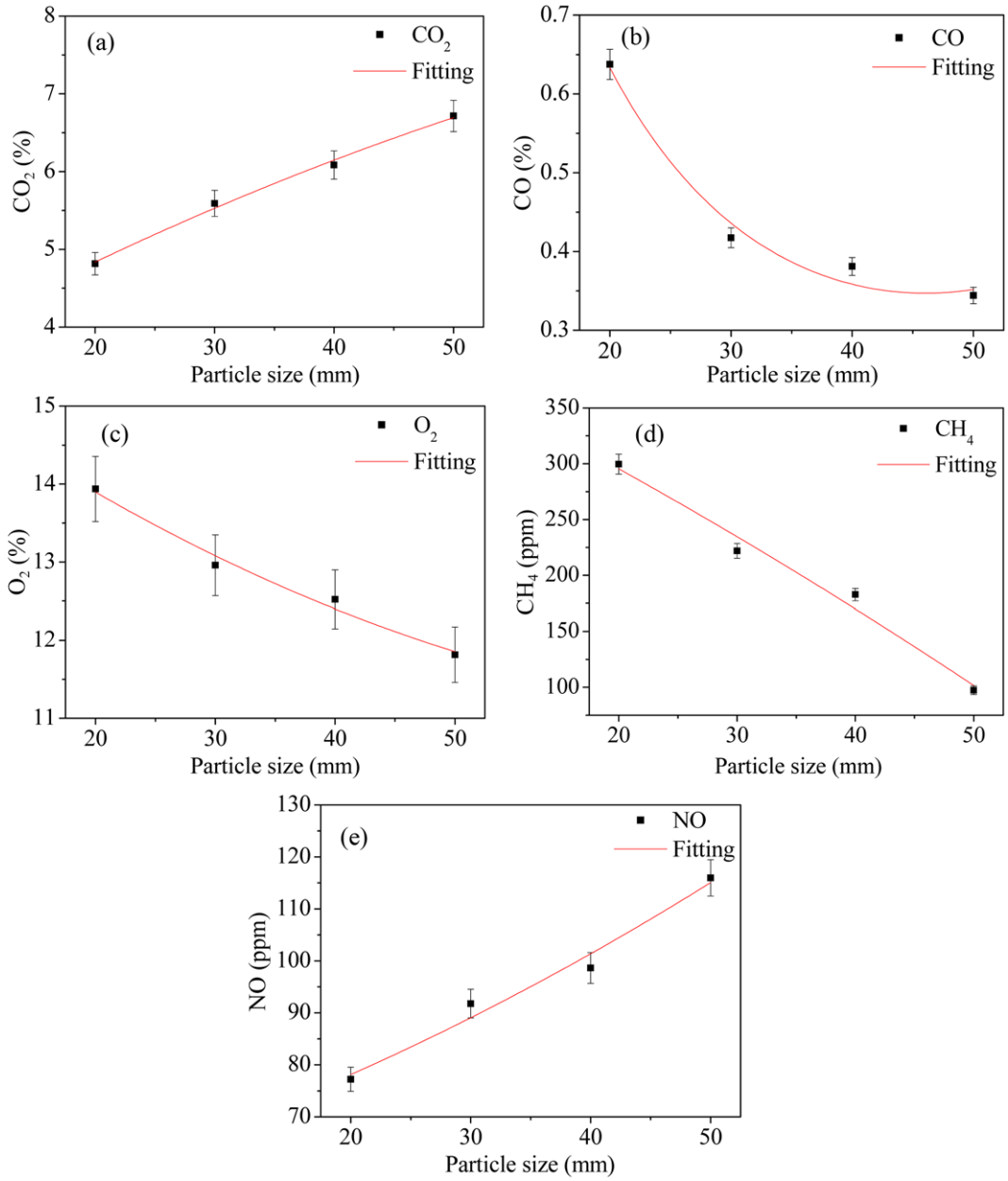

Fig. 9. The effect of particle size on combustion gases and NO.

introduced into the NO evaluation method. An expression for the average NO concentration between time t_1 and t_2 was developed and presented in Eq. (6).

Average CO_2 concentrations increased at first, reached a peak value at 14 Nm^3/h and finally decreased. In contrast, average CO concentrations decreased with increasing primary air rate. Average O_2 concentrations increased with increasing primary air rate while average CH_4 concentrations decreased initially, reached a minimum value and finally increased. The lowest NO concentrations were observed at 10 Nm^3/h. Primary air rates that are too high or too low elevate NO concentration levels. With increasing moisture content, concentrations of CO and CO_2 decreased while concentration of O_2 increased. CH_4 concentrations also decreased. A similar decreasing trend was obtained in NO concentrations. As bed height increased, CO_2 concentrations remained unchanged. All CO concentrations were observed with lower levels compared with those under different primary air rate conditions, but showed a decrease in CO concentrations with increasing bed height. CH_4 was observed to show a similar decreasing trend, average O_2 and NO concentrations in contradistinction increased with bed height. With increasing particle size, average concentrations of CO_2 increased nearly linearly and those of CO, CH_4 and O_2 decreased. The average concentration of NO increased with increasing particle size.

REFERENCES

1. C. J. Yang and C. Q. Hu, *Fuel Chem. Processes*, (in Chinese), **35**, 39 (2004).
2. T. H. Liou, *J. Hazard. Mater.*, **103**, 107 (2003).
3. R. Bassilakis, R. M. Carangelo and M. A. Wójtowicz, *Fuel*, **80**, 1765

(2001).
4. C.-L. Lin and M.-Y. Wey, *Korean J. Chem. Eng.*, **20**, 1123 (2003).
5. T. Chen, X. D. Li, J. H. Yan and Y. Q. Jin, *J. Hazard. Mater.*, **172**, 1339 (2009).
6. Y. F. Liu, *Chem. Eng. Design*, (in Chinese), **13**, 44 (2003).
7. X. H. Guan and G. M. Zhou, *Techniques and Equipment for Environmental Pollution Control*, **2**, 67 (2001).
8. Z. Q. Li, C. L. Liu, Z. C. Chen, J. Qian, W. Zhao and Q. Y. Zhu, *Bioresource Technol.*, **100**, 948 (2009).
9. W. P. Linak, C. A. Miller, D. A. Santoianni, C. J. King, T. Shinagawa, J. O. L. Wendt, J.-I. Yoo and Y.-C. Seo, *Korean J. Chem. Eng.*, **20**, 664 (2003).
10. Z. Q. Liu, J. H. Li and Y. F. Nie, *China Environ. Protection Ind.*, (in Chinese), **6**, 12 (2000).
11. Y. B. Yang, H. Yamauchi, V. Nasserzadeh and J. Swithenbank, *Fuel*, **82**, 2205 (2003).
12. C. Ryu, Y. B. Yang, A. Khor, N. E. Yates, V. N. Sharifi and J. Swithenbank, *Fuel*, **85**, 1039 (2006).
13. Y. B. Yang, V. N. Sharifi and J. Swithenbank, *Fuel*, **83**, 1553 (2004).
14. D. Shin and S. Choi, *Combust. Flame.*, **121**, 167 (2000).